

Chapter 8

Automated Optimization in HSPA Radio Network Planning

Iana Siomina, Di Yuan, and Fredrik Gunnarsson

Contents

8.1	Overview	272
8.2	Introduction	272
8.2.1	Background	272
8.2.2	HSPA Network Planning and Dimensioning	273
8.2.3	Chapter Scope	273
8.3	Modeling and Optimization	274
8.3.1	The System Model	275
8.3.1.1	Preliminaries and Overview	275
8.3.2	Coverage and CCH Power Consideration	278
8.3.3	R99 Power Consideration	279
8.3.4	HSDPA Performance	280
8.3.5	Uplink Consideration	281
8.4	Optimization Algorithm	283
8.4.1	Optimization Task	283
8.4.2	Complexity Consideration	283
8.4.3	Search Algorithms	284
8.4.4	Simulated Annealing	284
8.4.5	Configuration Adjustment	286

8.5 A Case Study 287

8.6 Conclusions..... 294

References 294

8.1 Overview

Automated optimization of radio network configurations can be considered a cost-effective means to improve mobile broadband performance, provided that accurate spatial network information is available. This chapter addresses automated optimization of antenna configurations in evolved 3G networks featuring High-Speed Packet Access (HSPA). Detailed radio link and network models are described, together with performance metrics in terms of link models relating radio link quality to data rates. The network planning task is formulated as an optimization problem maximizing HSDPA throughput with HSUPA performance as a soft constraint, while taking into account resource sharing among common channels, HSPA, and Release 99 traffic. A search algorithm is developed to solve the resulting optimization problem effectively and time efficiently. Performance analysis for a realistic large-scale planning scenario is provided to demonstrate the benefit of the automated optimization approach and the impact of optimizing different antenna configuration parameters, including antenna tilt and azimuth. For example, cell-edge data rates are improved by more than 50% by adopting automated optimization compared to the baseline configuration, and the largest performance gain is achieved by means of electrical antenna tilting.

8.2 Introduction

The increasing interest in mobile broadband services implies requirements on efficient data transport through radio networks. In part, this is handled by radio resource management mechanisms that dynamically adjust the network operations to cater for the current user needs. However, such mechanisms cannot fully compensate for poor network planning, which may substantially limit the potential radio network performance. An investment in careful radio network planning and network-wise configuration optimization is therefore well justified when it enables potentially greater revenues and improved user service experiences in the operational network.

8.2.1 Background

Radio networks of the third generation are continuously evolved by the 3rd Partnership Project (3GPP) specification work. A 3G network can be divided into a radio access network (RAN) and a core network (CN). The core network handles billing, higher layer services, data transport to other

networks, etc. The radio access network consists of one or several radio network subsystems (RNSs), each managed by a radio network controller (RNC). The actual radio links to the mobiles (or user equipment, UE) are maintained by base stations (or Node Bs).

In the first releases, both conversational and data services were mainly provided via dedicated channels (DCHs). A DCH is managed on a higher level by RNC, while Node B handles physical link operations, such as power control, to maintain an acceptable link quality. In addition, Node B transmits common channels (CCHs) to support other physical channels and handle connection initiations.

To enable faster and more flexible data transmissions to mobiles, HSDPA (High-Speed Downlink Packet Access) was introduced. Data for HSDPA users is carried over a shared channel, also called the high-speed downlink shared channel (HS-DSCH), and Node B decides which user to target with the channel (scheduling), and at what data rate (link adaptation). These decisions are based on feedback from UEs reporting the perceived radio channel quality.

Means to enable higher uplink data rates were also introduced as Enhanced Uplink (EUL) or High-Speed Uplink Packet Access (HSUPA). Similar to HSDPA, Node Bs are more involved in radio resource management. The combination of HSDPA and EUL/HSUPA is commonly referred to as High-Speed Packet Access (HSPA).

8.2.2 HSPA Network Planning and Dimensioning

A common tool in the planning and dimensioning process is a cell planning tool, typically featuring radio signal propagation prediction functionality. The accuracy of such predictions depends on the level of detail in the input information (terrain, land usage, buildings, antenna models, propagation models, expected services, traffic load, etc.), and also to what extent the models are adjusted to match the region considered in the planning procedure. If detailed information can be obtained, using optimization methods in the network planning phase becomes reasonable and beneficial.

In traditional network optimization with dedicated services, the focus is typically on the number of served users that are satisfied. Considering data transport over shared channels, such as HS-DSCH, different users will have different data rates. This calls for a modified set of key performance indicators. In particular, the focus shifts to data rate distributions, often with a special attention paid to performance-wise worst user locations.

8.2.3 Chapter Scope

The scope of the chapter is to introduce relevant models for HSPA planning and dimensioning, both with respect to common channels, dedicated

channels, as well as HSPA. In particular, performance metrics designed to address HSDPA performance take into account radio link quality as well as the scheduling strategy in Node B. Furthermore, various optimization algorithm considerations are discussed, including complexity and suitable search algorithms. A simulated annealing approach is described to optimize the antenna orientation parameters, and this approach is used to optimize a radio network in a case study.

8.3 Modeling and Optimization

Planning cellular networks deals with locating and configuring radio network elements to meet specified performance targets. Obtaining satisfactory results has to rely on some optimization process that approaches the planning problem systemically. This is a challenging engineering task, particularly for large-scale planning scenarios having many network elements, each with a large set of configuration parameters. In this context, an automated optimization engine, designed to tackle the complexity of large-scale planning with very little need for manual intervention or tuning, is highly desirable. The optimization engine alone, however, is not sufficient for accomplishing the planning task. Two additional key elements—system modeling and performance assessment—are equally important. In this chapter we practice a planning process formed by these three elements, as shown in Figure 8.1, to HSPA radio network planning.

Prior to system modeling, the scope of planning decisions is defined. Typically, the network planning stage deals with decisions that have significant mid-term and long-term impacts on performance, whereas decisions to respond to system dynamics, such as tuning handoff parameters and adjusting scheduling policies, lie in the domain of network operation. Major planning decisions include the location of base stations; antenna configuration in terms of height, tilt, and azimuth, coverage pattern; and for some cellular systems, channel assignment. Many of these decisions have

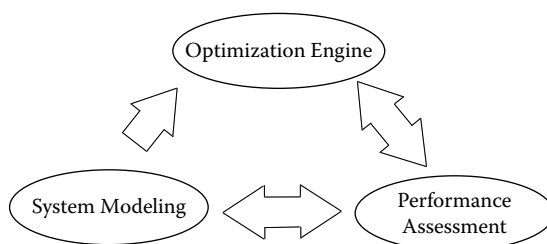


Figure 8.1 Key elements of an optimization process.

a multi-cell effect, even being applied in a single cell and, once taken, are costly to revise afterward; hence, the optimization process used in this stage is of vital significance.

System modeling translates the planning problem into a mathematical form based on expertise. The model identifies and quantifies how the performance indicators will respond to the design and configuration parameters considered in the planning (e.g., the effect of antenna tilting on signal-to-interference-plus-noise ratio (SINR)) and thereby data throughput. Typically and particularly for large-scale planning, the optimization process targets network-wise performance indicators. To this end, the goal of system modeling is to capture the essence of system behavior, rather than deriving an exact picture with full details, which, if doable at all, will result in planning problems that are too complex to be dealt with.

The optimization engine has the task of delivering a design solution. In this chapter the solution consists of tilt and azimuth configurations of cell antennas. The core of the engine is one or several optimization algorithms that are designed to produce high-quality solutions using a reasonable amount of computing effort. What is considered a reasonable amount varies from one planning case to another. For relatively easy planning problems, applying an off-the-shelf solver to a solution-oriented mathematical programming model [5] is a promising approach. For large-scale cellular network planning, however, stochastic search algorithms [4] are often more appropriate.

Performance assessment evaluates the optimization engine by numerical tests on planning scenarios with real-life or close-to-real-life data. In addition to the numerical values of the performance indicators reported by the optimization process, engineering expertise can be used to make a judgment of the planning solution and its performance from the practical point of view. Network simulation, if applicable to the planning scenario, is yet another useful tool for performance assessment. In addition to evaluating the optimization engine, performance assessment aims at analyzing the system model. The system model is revised accordingly if performance assessment identifies additional elements or constraints that are of significance to the overall performance. In the chapter, this aspect of performance assessment is illustrated by a comparative study of the impact of uplink consideration in HSPA planning.

8.3.1 The System Model

8.3.1.1 Preliminaries and Overview

For HSDPA, data throughput is the primary performance consideration. Several factors influence the downlink user data throughput: the SINR, the number of channelization codes, and resource sharing decisions, in

particular scheduling. Among them, SINR is the key performance aspect from a network planning viewpoint. The SINR of HS-DSCH is a result of radio propagation condition, interference, noise, and transmission power. Although SINR is of primary concern in implementing both 3GPP Release 99 (R99) and HSDPA services, there is a significant difference in system modeling, namely that the closed-loop power control on the R99 DCH does not apply to HS-DSCH. Thus, HSDPA users will enjoy higher data throughput by more power at downlink.

The system model in this chapter accounts for networks with coexisting R99 and HSDPA. For this type of planning scenario, the output power of Node B is shared between HS-DSCH, DCH, and CCH, including common pilot channel (CPICH) defining network coverage and cell ranges. A common power-sharing strategy is the fill-up approach [11], which allocates all the power left from supporting CCH and DCH to HS-DSCH. By this approach, HSDPA power is dynamic, yielding better resource utilization in comparison to a constant amount of HS-DSCH power. As a result of the fill-up approach, the cells constantly operate at full power at the downlink in the system model.

The two planning parameters in the optimization framework, tilt and azimuth, refer to the angle of the main beam of the antenna below the horizontal plane (downtilt), and the horizontal angle between the north and the antenna's main lobe direction, respectively. For tilting, mechanical tilting, electrical tilting, as well as their combinations are considered. With mechanical tilting, the physical angle of the brackets used to mount the antenna is adjusted, while with electrical tilting, the antenna pattern is adjusted by varying the weights of antenna elements. As no physical adjustment is required, electrical tilting can be controlled remotely and is therefore a more cost-effective way of reducing interference.

Denote by $\mathcal{C} = \{1, \dots, C\}$ the set of cells, where C is the number of cells. The total transmission power available in cell $i \in \mathcal{C}$ is denoted by P_i^{TOT} . To simplify the discussion, we consider one directional antenna in every cell. In the subsequent text, the two terms (antenna and cell) are often used interchangeably. The configuration of antenna i is a tuple $\langle t_i^m, t_i^e, a_i \rangle$, where t_i^m , t_i^e , and a_i are the mechanical tilt, electrical tilt, and azimuth angles, respectively. Each of the three parameters has a discrete set of candidate values. For antenna i , all possible combinations of the three parameter values form a set of candidate configurations $\mathcal{K}_i = \{1, \dots, K_i\}$. The network-wise antenna configuration is a vector $\mathbf{k} = (k_1, \dots, k_C)$, where $k_i \in \mathcal{K}_i$ is the configuration of antenna i .

The service area is modeled by a regular grid of pixels $\mathcal{J} = \{1, \dots, J\}$, where J is the number of pixels. A pixel $j \in \mathcal{J}$ is a small square area within which radio propagation is considered uniform in the network planning context. Higher pixel resolution yields more accurate planning, at the

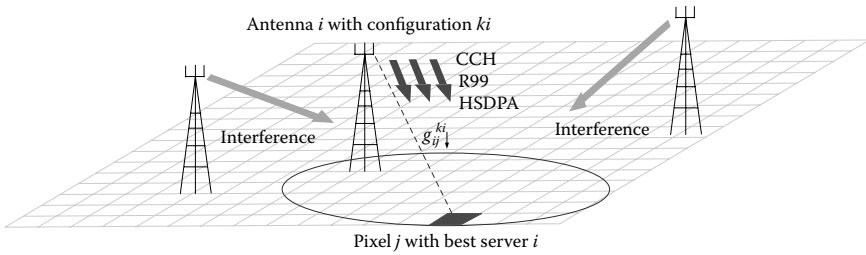


Figure 8.2 An illustration of some elements of the planning framework.

price of increasing the size of the planning problem. We use $g_{ij\downarrow}^{k_i}$ and $g_{ij\uparrow}^{k_i}$ to denote the total average power gain between antenna i under configuration k_i and pixel j at downlink and uplink, respectively. The gain values are defined by environment-dependent signal propagation conditions, hardware characteristics (e.g., maximum antenna gain, directional antenna losses, cable loss, body loss, etc.), and depend also on configuration (e.g., antenna tilt and azimuth). The number of candidate antenna configurations and pixel resolution together set the amount of data required for planning. In Figure 8.2, we provide an illustration of some concepts and elements that have been introduced.

For a user demand map (i.e., distribution of active users of each service type), let $P_i^{CCH}(\mathbf{k})$, $P_i^{DCH}(\mathbf{k})$, and $P_i^{HS}(\mathbf{k})$ denote the power consumed by CCH, DCH, and HS-DSCH in cell i , respectively, under network antenna configuration \mathbf{k} . We have

$$P_i^{TOT} = P_i^{CCH}(\mathbf{k}) + P_i^{DCH}(\mathbf{k}) + P_i^{HS}(\mathbf{k}), \quad i \in \mathcal{C} \quad (8.1)$$

Figure 8.3 gives an overview of the components in the optimization framework. Given an antenna configuration vector, we compute the power needed on CCH for coverage and the best server pattern, that is, the serving antenna of each pixel. The best server pattern and the R99 user demand map determine the downlink power consumed by R99. This, together with the power on CCH, give the HS-DSCH power of each cell by Equation (8.1). The achievable HSDPA data throughput over the service area can then be computed from the HS-DSCH power, the antenna configuration, and a given HSDPA demand map. In the following sections we detail the relationship between the system components in Figure 8.3.

As shown in Figure 8.3, the evaluation of HSDPA performance uses R99 and HSDPA demand maps as input. A demand map corresponds to a snapshot of the users served by the network over the service area. To achieve a robust solution in antenna configuration, the optimization can be

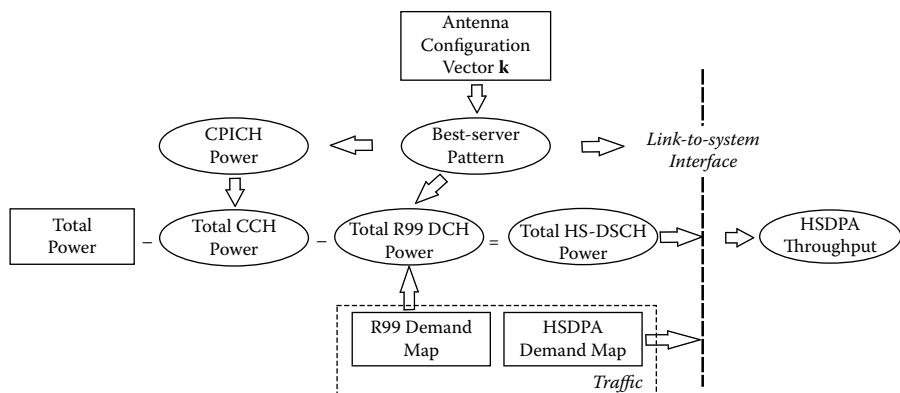


Figure 8.3 Downlink components in the optimization framework.

performed for a large number of demand maps following expected user distribution, or for an aggregated statistical demand map of each traffic type.

8.3.2 Coverage and CCH Power Consideration

Network coverage is provided by the presence of CPICH [2]. CPICH enables UE to perform channel estimation and cell selection/reselection. The requirement of CPICH presence can be modeled by $E_c/I_0 \geq \gamma^c$, where E_c/I_0 is the ratio between the received chip energy and the total received power spectral density at the UE's antenna connector [1], and γ^c is a threshold value. CPICH E_c/I_0 over the service area is a result of antenna configuration and CPICH power allocation. At present, a common practice is the uniform scheme, that is, to allocate the same amount of power to CPICH in all cells, which is therefore further assumed in the chapter. Nonuniform CPICH power has been studied, for example, in [18]. Let $P^{CPICH}(\mathbf{k})$ denote the CPICH power for configuration \mathbf{k} , and v_\downarrow the total noise power in downlink. Under antenna configuration vector \mathbf{k} , antenna i covers pixel j with CPICH if the following inequality holds:

$$E_c/I_0 = \frac{P^{CPICH}(\mathbf{k})g_{ij\downarrow}^{k_i}}{\sum_{l \in \mathcal{C}} P_l^{TOT} g_{lj\downarrow}^{k_l} + v_\downarrow} \geq \gamma^c \quad (8.2)$$

Because CPICH is transmitted continuously, an excess power level of CPICH makes less power available to traffic channels and may also cause pilot pollution. Thus, the goal is to find the minimum level of $P^{CPICH}(\mathbf{k})$ to ensure the coverage of the service area. From Equation (8.2), coverage

at j is secured only if $P^{CPICH}(\mathbf{k}) \geq \min_{i \in \mathcal{C}} (\sum_{l \in \mathcal{C}} P_l^{TOT} g_{lj\downarrow}^{k_l} + v_{\downarrow}) \gamma^c / g_{ij\downarrow}^{k_i}$. To cover all $j \in \mathcal{J}$, the required CPICH power is therefore [19]

$$P^{CPICH}(\mathbf{k}) = \max_{j \in \mathcal{J}} \min_{i \in \mathcal{C}} \frac{\left(\sum_{l \in \mathcal{C}} P_l^{TOT} g_{lj\downarrow}^{k_l} + v_{\downarrow} \right) \gamma^c}{g_{ij\downarrow}^{k_i}} \quad (8.3)$$

In addition to CPICH, power must be allocated to other common channels, for example, synchronization channel (SCH), paging indicator channel (PICH), and acquisition indicator channel (AICH). These common channels are typically powered in proportion to CPICH [14]. In the system model, the total power consumed by CCHs is estimated by scaling $P^{CPICH}(\mathbf{k})$ with a factor $\beta > 1$,

$$P_i^{CCH}(\mathbf{k}) = \beta P^{CPICH}(\mathbf{k}), \quad i \in \mathcal{C} \quad (8.4)$$

If a pixel $j \in \mathcal{J}$ is covered by the CPICH of multiple antennas, the one giving the highest E_c/I_0 is referred to as the best server. Equivalently speaking, the best server is the antenna having the largest gain value in j , because the numerator in Equation (8.3) is a constant for a given antenna configuration vector \mathbf{k} . Thus, there is a straightforward mapping between antenna configuration and the best server pattern. In the following, $\mathcal{J}_i(\mathbf{k})$ denotes the subset of pixels for which antenna i is the best server under configuration \mathbf{k} .

8.3.3 R99 Power Consideration

Denote by \mathcal{S} the set of service types in R99. Each service $s \in \mathcal{S}$ is characterized by its SINR target γ^s and an activity factor v^s . The R99 demand map is specified by the number of admitted users in each pixel and of each service type, denoted by d_{js}^{DCH} , $j \in \mathcal{J}$, $s \in \mathcal{S}$. For each user of service type s , closed-loop power control strives to meet the SINR target γ^s . For antenna i and pixel j served by i (i.e., $j \in \mathcal{J}_i(\mathbf{k})$), denote by P_{ijs}^{DCH} the power consumed by supporting a user in j of service type s . Let α_j denote the orthogonality factor in j (with $\alpha_j = 1$ modeling full orthogonality, that is, no intra-cell interference). Under perfect power control, $P_{ijs}^{DCH}(\mathbf{k})$ can be obtained from the following equation:

$$\frac{P_{ijs}^{DCH}(\mathbf{k}) g_{ij\downarrow}^{k_i}}{(1 - \alpha_j) (P_i^{TOT} - v^s P_{ijs}^{DCH}(\mathbf{k})) g_{ij\downarrow}^{k_i} + \sum_{l \in \mathcal{C}: l \neq i} P_l^{TOT} g_{lj\downarrow}^{k_l} + v_{\downarrow}} = \gamma^s. \quad (8.5)$$

In Equation (8.5), the inter-cell interference is calculated under total cell power at downlink, and lower activity factor gives higher intra-cell

interference. Both are consequences of Equation (8.1). To provide service to the R99 users located in $\mathcal{J}_i(\mathbf{k})$, the DCH power of antenna i is

$$P_i^{DCH}(\mathbf{k}) = \sum_{j \in \mathcal{J}_i(\mathbf{k})} \sum_{s \in \mathcal{S}} d_{js}^{DCH} v^s P_{ijs}^{DCH}(\mathbf{k}), \quad i \in \mathcal{C} \quad (8.6)$$

The power vector given by Equation (8.6) corresponds to the downlink load factor—one of the key performance indicators in a network based on WCDMA (wideband code division multiple access) [12]. For this reason, it is typically incorporated into the objective function in automated optimization for planning R99 networks [16]. For networks with both R99 and HSDPA services, it is reasonable to assume that, by R99 admission control, the R99 demand map will not lead to a DCH power consumption exceeding some specified percentage of the total cell power. Thus, some power will always be available to HSDPA data.

8.3.4 HSDPA Performance

From Equation (8.1), the power of HS-DSCH in cell i is $P_i^{HS}(\mathbf{k}) = P_i^{TOT} - P_i^{CCH}(\mathbf{k}) - P_i^{DCH}(\mathbf{k})$. Denote by $d_j^{HS}(j \in \mathcal{J})$ the number of active users in j in the HSDPA demand map. In addition to power and interference, throughput on HS-DSCH depends on several factors, such as the modulation scheme and the number of channelization codes. To model HSDPA performance, a suitable SINR metric is the narrowband SINR ratio after despreading the HS-PDSCH (High-speed Physical Down-Link Shared Channel) [7]. For antenna i and pixel $j \in \mathcal{J}_i(\mathbf{k})$, this SINR value reads:

$$SINR_{ij}^{HS}(\mathbf{k}) = SF^{HS} \times \frac{P_i^{HS}(\mathbf{k})}{P_i^{TOT} \left(1 - \alpha_j + \frac{I_{oc}}{I_{or}} \right)} \quad (8.7)$$

In Equation (8.7), $I_{oc} = \sum_{l \in \mathcal{C}: l \neq i} P_l^{TOT} g_{lj\downarrow}^{k_l} + v_\downarrow$ is the received other-cell interference plus noise, and $I_{or} = P_i^{TOT} g_{ij\downarrow}^{k_i}$ is the received power from the serving cell i . The spreading factor SF^{HS} equals 16. Note that the definition of Equation (8.7) does not depend on the number of channelization codes or the modulation scheme. A function $\phi(SINR_{ij}^{HS})$ is then used to translate $SINR_{ij}^{HS}$ into single-user data throughput (bps), taking into account the effect of the number of codes, AMC (adaptive modulation and coding), and HARQ (Hybrid Automatic Repeat Request). The shape of function ϕ can be obtained empirically [7]. Merely for the sake of simplifying notation, consider the case where ϕ is of the same shape for all users (extension to user-specific mobility profile and number of codes is straightforward).

Then the average HSDPA single-user data throughput can be expressed as

$$\bar{\phi}(\mathbf{k}) = \frac{\sum_{i \in \mathcal{C}} \sum_{j \in \mathcal{J}_i(\mathbf{k})} d_j^{HS} \cdot \phi(\text{SINR}_{ij}(\mathbf{k}))}{\sum_{j \in \mathcal{J}} d_j^{HS}} \quad (8.8)$$

It is worth noting that parameters d_j^{HS} , $j \in \mathcal{J}$ do not necessarily have to represent a specific HSDPA user demand map. Instead, these parameters can be used as weights to reflect the relative importance of different parts of the service area. For example, setting $d_j^{HS} = 1$, $j \in \mathcal{J}$, $\bar{\phi}(\mathbf{k})$ models the average single-user throughput over the entire service area. For planning scenarios where cell-edge throughput is of primary concern, zero weight can be assigned to pixels other than the ones forming cell edges.

In addition to single-user throughput, another interesting performance metric is the HSDPA cell-average throughput. In this case, the behavior of the Node B scheduler, which controls the time sharing among all simultaneously active users in a cell, should be accounted for. Two commonly used scheduling schemes are Round Robin (RR) and Proportional Fair (PF). Denote by τ_j the time share of a user in $j \in \mathcal{J}_i(\mathbf{k})$. Under RR scheduling, all users in $\mathcal{J}_i(\mathbf{k})$ have equal time share, whereas in PF scheduling the time allocated to a user in j is proportional to its channel condition, reflected by $\phi(\text{SINR}_{ij}^{HS})$. Hence, parameters τ_j for the two scheduling schemes, respectively, take the form

$$\tau_j = \frac{1}{\sum_{j \in \mathcal{J}_i(\mathbf{k})} d_j^{HS}} \quad \text{and} \quad \tau_j = \frac{\phi(\text{SINR}_{ij}^{HS}(\mathbf{k}))}{\sum_{j \in \mathcal{J}_i(\mathbf{k})} d_j^{HS} \cdot \phi(\text{SINR}_{ij}(\mathbf{k}))} \quad (8.9)$$

Let $\Phi_i(\mathbf{k})$ denote the average HSDPA throughput of cell i , and define cell-average throughput $\Phi(\mathbf{k}) = \frac{1}{C} \sum_{i \in \mathcal{C}} \Phi_i(\mathbf{k})$. Given a scheduling strategy, $\Phi_i(\mathbf{k})$ can be computed by the following expression:

$$\Phi_i(\mathbf{k}) = \frac{\sum_{j \in \mathcal{J}_i(\mathbf{k})} d_j^{HS} \cdot \phi(\text{SINR}_{ij}(\mathbf{k})) \cdot \tau_j}{\sum_{j \in \mathcal{J}_i(\mathbf{k})} d_j^{HS}} \quad (8.10)$$

8.3.5 Uplink Consideration

Given antenna configuration k_i of cell i , the uplink SINR requirement for user j being provided service s in cell i can be formulated as follows:

$$\frac{p_j g_{ji\uparrow}^{k_i}}{\sum_{j' \in \mathcal{J}: j' \neq j} \omega_{j'} p_{j'} g_{j'i\uparrow}^{k_i} + \nu_{\uparrow}} \geq \gamma^s \quad (8.11)$$

where p_j is the transmission power of a user in pixel j , $g_{ji\uparrow}^{k_i}$ is the total power gain between a user transmitter in pixel j and the cell i receiver, $\omega_{j'}$ is the activity factor in pixel j' , and v_{\uparrow} is the total noise power received at Node B antenna i . To simplify the formulation, we assume the same noise power at all Node Bs and the same SINR threshold as in the downlink. Note that the activity factor $\omega_{j'}$ takes into account the service s activity, the number of users in pixel j' , and the single-user activity in the pixel. Assuming the maximum UE power p^{max} and a known noise-rise factor $r_i(\mathbf{k})$ in cell i , the following condition necessary to provide service s in pixel j can be derived from Equation (8.11):

$$g_{ji\uparrow}^{k_i} \geq \frac{\gamma^s}{1 + \omega_j \gamma^s} \cdot \frac{r_i(\mathbf{k}) v_{\uparrow}}{p^{max}} \quad (8.12)$$

where $r_i(\mathbf{k}) = \frac{1}{v_{\uparrow}} \cdot \left(\sum_{j' \in \mathcal{J}} \omega_{j'} p_{j'} g_{ji\uparrow}^{k_i} + v_{\uparrow} \right)$. In detailed planning, noise-rise factors for a given antenna configuration vector \mathbf{k} can be found by solving the following system of C linear equations (see, e.g., [16]):

$$\left(1 - \sum_{j \in \mathcal{J}_i(\mathbf{k})} \frac{w_j \gamma^s}{1 + w_j \gamma^s} \right) r_i(\mathbf{k}) - \sum_{l \in \mathcal{C}: l \neq i} \left(\sum_{j \in \mathcal{J}_l(\mathbf{k})} \frac{g_{ji\uparrow}^{k_i} w_j \gamma^s}{g_{jl\uparrow}^{k_l} (1 + w_j \gamma^s)} \right) \times r_l(\mathbf{k}) = 1, \quad i \in \mathcal{C} \quad (8.13)$$

In some cases the network can be dimensioned and configured for a given maximum noise-rise factor r^{max} , that is, assuming $r_i(\mathbf{k}) = r^{max}$, $i \in \mathcal{C}$. The approach can be used for higher-level planning, in situations with high traffic variation or uncertainties, and can also be adopted for HSUPA assuming that data is always available for transmission.

In radio network planning and optimization, there is often a target coverage degree ξ . With the presented uplink model, the uplink coverage degree $\xi(\mathbf{k})$ for antenna configuration \mathbf{k} is the fraction of the total service area where the coverage condition of Equation (8.12) is satisfied for all services for the found noise-rise factors. The antenna configuration is said to provide the desired UL coverage when the fraction is at least ξ , otherwise an UL coverage loss of $\xi - \xi(\mathbf{k})$ occurs. In practice, the coverage requirement can be service specific, which is a straightforward extension to the presented model.

8.4 Optimization Algorithm

8.4.1 Optimization Task

To tackle a planning problem, the optimization engine needs as input a system model that captures the system behavior depending on the decision variables, and an optimization task specified as a set of objectives and constraints. The system model in the previous sections links antenna configuration \mathbf{k} (a vector of decision variables) to HSDPA performance metrics $\bar{\phi}(\mathbf{k})$ and $\Phi(\mathbf{k})$. The former does not depend on the assumption of the scheduling policy, and for this reason it will be used as the objective function to illustrate the optimization process. The optimization task is hence to solve the combinatorial optimization problem of *finding an antenna configuration that maximizes $\bar{\phi}(\mathbf{k})$* :

$$\max_{\mathbf{k} \in \mathcal{K}_1 \times \dots \times \mathcal{K}_C} \bar{\phi}(\mathbf{k}) \quad (8.14)$$

The desired UL coverage is introduced as a soft constraint with which the optimization task can be reformulated as *finding an antenna configuration that maximizes $\bar{\phi}(\mathbf{k})$ while minimizing the UL coverage loss $\xi - \xi(\mathbf{k})$* . The new objective function is $F(\mathbf{k}) = \bar{\phi}(\mathbf{k}) (1 - \rho \cdot \max\{\xi - \xi(\mathbf{k}), 0\})$, where the introduced weighted penalty makes configurations with a coverage loss of at most $1 - \xi$ preferred, and those with a higher loss feasible but left for a later judgment.

8.4.2 Complexity Consideration

From a computational complexity viewpoint, the problem in (8.14) is *NP*-hard and no more difficult than that with the coverage loss penalty in the objective function; a formal proof of this result can be obtained from a generalization of the 3-satisfiability problem, of which the *NP*-hardness is well known [8]. *NP*-hardness is a term used to denote a class of computationally difficult optimization problems. It implies that an algorithm guaranteeing global optimum will take, in the worst case, an amount of computing time growing exponentially in the problem size. In (8.14), the problem size is defined by the number of candidate configurations at each antenna and the number of pixels used to represent the service area. The hardness of the problem and the objective of dealing with large-scale planning scenarios justify the use of heuristic search algorithms, which, although do not guarantee optimality, are effective in finding high-quality solutions quickly.

8.4.3 Search Algorithms

There is a rich set of principles that have been developed for designing search algorithms, such as local search [4], tabu search [9], simulated annealing [13], greedy randomized adaptive search procedure (GRASP) [17], and genetic algorithms [10]. The general idea, shared by all the algorithms, is to perform an iterative search in the solution space. The objective function is used to drive the search toward better solutions. In every iteration, one solution (or a set of solutions) is kept, and a set of new solutions, generated by modifying parts of the current one, are evaluated. The scheme used for solution modification is hence a key algorithmic design aspect. The current solution is replaced by a new one, if the latter has a better performance value. For many search algorithms, this update operation is referred to as a move in the solution space. Taking solution-improving moves will eventually end up at a local optimum, that is, a solution for which the modification scheme is not able to improve, but it is not necessarily the global optimum. To deal with this issue, all algorithms, except local search, implement some mechanism to drive the search from local optima, by temporarily accepting moves leading to worse solutions. For tabu search, the mechanism is to allow only moves that tend to go away from local optima. The other algorithms incorporate randomization to achieve a similar effect.

To design a search algorithm for (8.14), the most natural way of solution modification is to adjust the tilt and/or azimuth angles of one or several antennas. Thus, a general recipe of algorithmic design has the following key components:

1. Configuration adjustment of one or several antennas
2. Performance evaluation by the system model
3. Solution update

In the rest of this section, an implementation of the recipe is demonstrated through a simulated annealing algorithm.

8.4.4 Simulated Annealing

A simulated annealing algorithm generates and evaluates one solution per iteration. It adopts a probabilistic move to deal with local optima. Suppose \mathbf{k} is the current antenna configuration, and \mathbf{k}' is a new configuration from adjustment of \mathbf{k} . If the objective function improves, that is, $F(\mathbf{k}') > F(\mathbf{k})$, the algorithm moves to \mathbf{k}' . Otherwise, the move is made with a probability. The standard function for determining the probability is $e^{-\delta/T}$. Here, δ is the amount of worsening in solution performance, that is, $F(\mathbf{k}) - F(\mathbf{k}')$ or the relative difference $(F(\mathbf{k}) - F(\mathbf{k}')) / F(\mathbf{k})$. The denominator T , called temperature, is a parameter used by the algorithm to control the willingness of accepting the worsening. By the probability function, it is more likely to

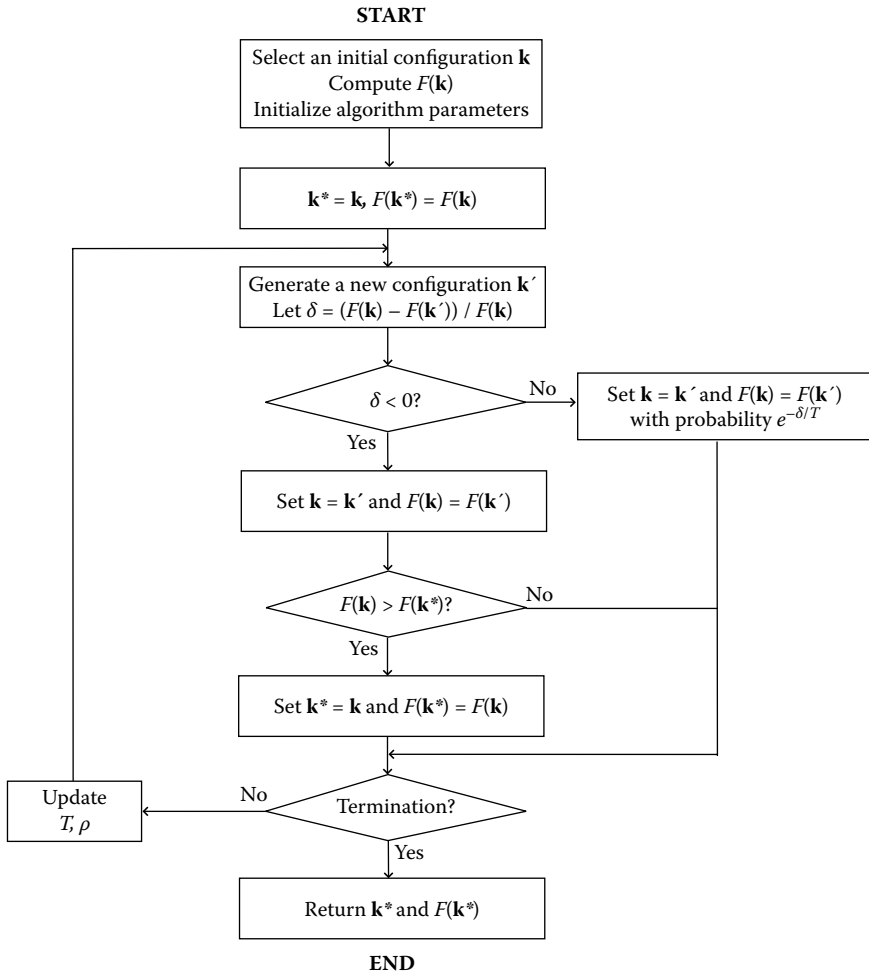


Figure 8.4 A flowchart of the optimization algorithm.

move to a worse solution if $F(\mathbf{k}) - F(\mathbf{k}')$ is small or T is large. The algorithm stops after a maximum allowed number of iterations, of which the value is set to make the computation time-affordable. Parameter T should be high enough at the algorithm start to enable moving away from local optima. During the search, the value of T and consequently the probability of accepting non-improving moves decrease gradually. Typically, T approaches zero when the number of performed iterations gets close to the maximum allowed number. To control the importance of the soft UL coverage constraint, the weighting factor ρ in the objective function is increased after every new move with $\xi - \xi(\mathbf{k}') > 0$, and decreased otherwise. The flowchart of the algorithm is given in Figure 8.4.

8.4.5 Configuration Adjustment

The algorithm design is not complete without specifying how to generate a new configuration vector \mathbf{k}' from \mathbf{k} . The most obvious choice is to randomly select an antenna i , and pick a configuration k'_i , again randomly, from $\mathcal{K}_i \setminus \{k_i\}$. Vector \mathbf{k}' then takes the form $(k_1, \dots, k_{i-1}, k'_i, k_{i+1}, \dots, k_C)$. This type of purely random selection is, however, not effective; too often, it produces \mathbf{k}' that performs worse than \mathbf{k} . Because the time required to evaluate a configuration vector grows by network size, for large-scale planning it becomes crucial that configuration adjustment will frequently yield solution improvement.

A refined strategy, in which configuration adjustment is restricted to a few cells that appear to be critical to HSDPA throughput under current configuration \mathbf{k} , turns out to be very effective in exploring the solution space. The underlying idea is to consider one of the pixels having lowest SINR and hence poor throughput, and a small subset of cells having largest impact on this SINR value. Let j be the pixel under consideration. The set of critical cells is composed by the best server and the cells generating heavy interference, that is, cells having highest gain values in j (cf. the scenario illustrated by Figure 8.2). Each critical cell receives a value representing its importance, set in proportion to the gain. The algorithm selects a cell from the critical set, with a probability distribution following the cells' relative importance values. Once a cell is selected, one of its alternative candidate configurations is chosen randomly. The SINR at j is then reevaluated. Because this evaluation is made for j only, it demands very little computation. The algorithm makes a number of such minor iterations, each of which is a reconfiguration trial of one critical cell for j . The output configuration is the one giving the highest SINR at j . This output configuration defines \mathbf{k}' in the major algorithm iteration.

Although possible antenna adjustments are very restricted per iteration in the above procedure, diversity is not lost. The pixel used for defining critical cells varies by \mathbf{k} . As a result, the set of cells subject to configuration adjustment will move from one part of the network to another during the search.

8.5 A Case Study

As a case study for the presented optimization framework, we consider a test network originating from a planning scenario for the downtown area of Lisbon, provided by the MOMENTUM project [3]. The network parameters are summarized in Table 8.1. Given isotropic pathloss predictions [3] and antenna diagrams, the power gain parameters for each antenna configuration have been found by the model in [6]. An antenna configuration in

Table 8.1 Network Parameters

<i>Parameter</i>	<i>Value</i>
Number of sites/cells (C)/pixels (J)	60/164/52500
Pixel size	20 m \times 20 m
Total service area size	4200 m \times 5000 m
Total cell transmission power (P_i^{TOT} , all cells)	20 W
Total downlink noise power (v_{\downarrow})	8×10^{-14} W
Total uplink noise power (v_{\uparrow})	4×10^{-14} W
Downlink installation loss	3 dB
Node B antenna	Kathrein K742265, 2110 MHz, 18.5 dBi
UE antenna	omni, 0 dB
Maximum UE power (p^{max})	0.2 W
Total downlink CCH power/CPICH power (β)	1.8
CPICH E_c/I_0 target (γ^c)	0.01
SINR target for R99 speech (γ^{speech})	5.5 dB
UL target coverage degree (ξ)	0.95

this study is a combination of antenna electrical tilt, mechanical tilt, and azimuth. For each tilt type, the range of possible values is from 0° to 6° . Because the studied network represents an urban environment with dense site locations (typically interference limited), the preference in downtilting is given to electrical tilting, that is, mechanical downtilt can be used only if electrical downtilt has reached its 6° maximum. Antenna azimuth can be adjusted in the range of $[-10^\circ, +10^\circ]$ with a 5° step. An installation loss of 3 dB is assumed in downlink, but not in uplink, for which we assume tower-mounted amplifiers. The UL coverage is evaluated over a statistical snapshot of the entire area; the snapshot mimics nonuniform user distribution while still accounting for the contribution of every pixel.

Five antenna configurations are considered for performance evaluation. In the reference configuration (REF), 2.0 W CPICH power, no tilt, and default azimuth are assumed. In the optimized configurations, the CPICH power is to be found together with network antenna configuration \mathbf{k}^* , where the optimization decision space is given by the range of either a single antenna parameter (electrical tilt in ET, mechanical tilt in MT, or azimuth

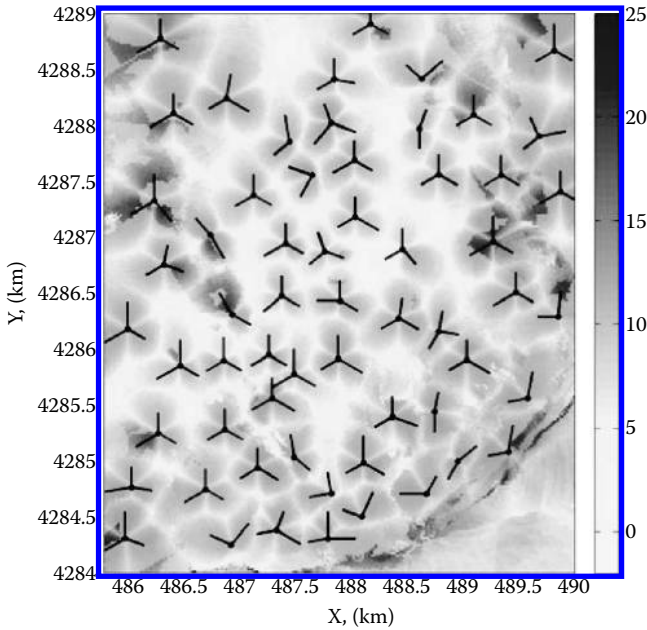


Figure 8.5 HS-DSCH SINR in REF configuration, (dB).

in AZ configuration) or all three parameters (MEA configuration). For each of the configuration scenarios, the optimization algorithm has been run for a statistical user distribution snapshot of R99 traffic for which we assume speech service with an activity factor $v^{speech} = 0.5$ and an SINR target of 5.5 dB. The orthogonality factor is nonuniform and has been provided together with the data. The assumed HSDPA service demand and user activity factors in UL are uniform, which is not a limitation of the presented framework, but allows us to obtain a generic solution independent of HSDPA traffic distribution and scheduling.

Node B locations and initial antenna configuration are depicted in Figure 8.5 where we also show HS-DSCH SINRs over the service area in REF configuration. The SINR distribution gives us a general picture of system performance without the need to consider any specific HS-user distribution or mapping function ϕ . Figure 8.6 and Figure 8.7 demonstrate the SINR distribution and HSDPA throughput, respectively, in MEA configuration, for which the largest improvement among all configurations has been achieved due to more configuration alternatives. For throughput mapping we used a function in [11] obtained by simulations for five channelization codes and the Pedestrian-A mobility model. We observe that optimizing antenna configurations allows us to achieve better cell isolation between

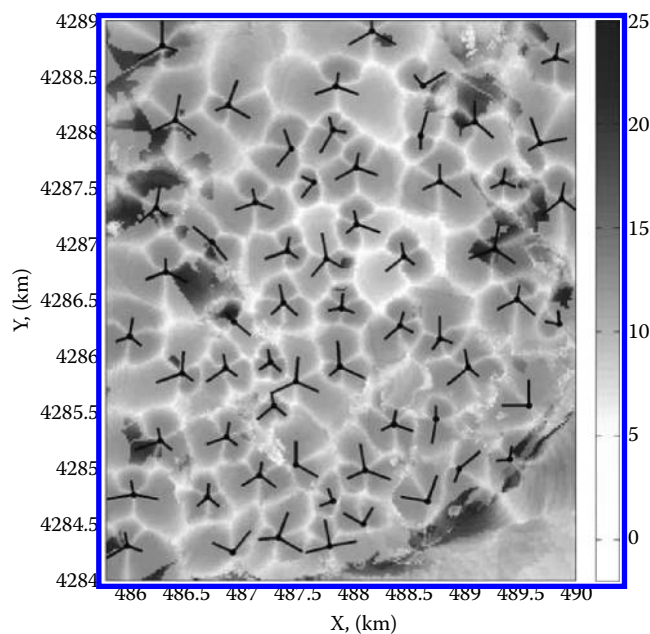


Figure 8.6 HS-DSCH SINR in MEA configuration, (dB).

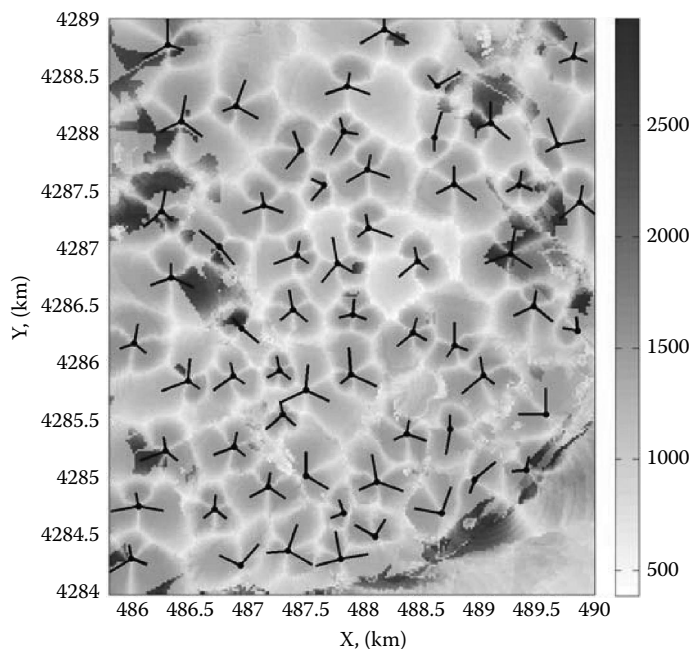


Figure 8.7 HSDPA throughput in MEA configuration, (kbps).

densely located sites and improve the received signal quality in areas with bad coverage. The difference is particularly significant in areas having low signal quality in REF antenna configuration, that is, areas where an increase in throughput gives more perceived service enhancement.

To evaluate HSDPA performance for a realistic HSDPA user distribution, we consider a snapshot with 2,380 active users nonuniformly distributed over the service area. Table 8.2 summarizes the power and coverage statistics for the five configurations. Table 8.3 summarizes the single-user and cell HSDPA throughput. In both tables, when relevant, we show the mean, and the 5th and 95th percentile values of the performance metrics. The last row in each table shows the maximum relative change (in %) obtained by optimization, that is, comparing MEA and REF configurations. A great reduction in uniform CPICH and thus CCH power can be observed in all scenarios. The improved interference also results in less power needed to support R99 traffic in the optimized configurations and therefore overall more power available for HSDPA traffic. The relative power budget improvement for HSDPA is, however, smaller than the relative gains in CCH and R99 power due to their smaller total weight in the cell power budget. The maximum (over all configurations) relative cell throughput improvement is approximately in the same range as the HSDPA power budget gain, although slightly higher for RR scheduler which is more sensitive to poor performance of cell-edge users. As expected, the largest difference between the two schedulers (8.5%) is in the fifth percentile, for which the single-user throughput improvement is also the largest. In a sense, the PF scheduler can be seen as a radio resource management means to improve cell-edge data rates compared to using RR. With the REF configuration, the fifth percentile data rate is increased by 7.4% when using PF compared to RR. In a better planned MEA, the fifth percentile data rate is increased by only 1.7%. Hence, the relative impact of more advanced radio resource management mechanisms is greater for worse planned networks. In other words, in well-planned networks, there may be less need for advanced radio resource mechanisms to provide good cell-edge data rates.

As already discussed, MEA configurations have the best performance among the five configurations. Among the configurations optimized for a single antenna parameter, the best performance is achieved with electrical tilting, which is the most effective way of reducing inter-cell interference, while AZ gives least performance gain because changing antenna azimuth just shifts interference, which may be inefficient in environments with densely located sites. Another observation is that ET configuration performance is very close to that of MEA; this is due to the effect of the soft UL coverage constraint, which prioritizes solutions with no excessive UL coverage loss. Note also that the target UL coverage has been achieved with all optimized configurations, but not in REF.

Table 8.2 Power and Coverage Statistics

<i>Configuration</i>	<i>UL Coverage (%)</i>	<i>CCH Power (W)</i>	<i>R99 Power, (W)</i>			<i>HSDPA Power, (W)</i>		
			<i>5%</i>	<i>95%</i>	<i>Mean</i>	<i>5%</i>	<i>95%</i>	<i>Mean</i>
REF	91.54	3.60	0.38	8.11	3.05	8.17	15.90	13.30
MT	95.73	1.80	0.31	5.94	2.38	12.16	17.82	15.78
ET	96.99	1.71	0.26	5.59	2.17	12.59	17.97	16.08
AZ	95.86	2.41	0.38	7.99	3.02	9.22	17.06	14.52
MEA	97.37	1.46	0.23	5.63	2.11	12.83	18.21	16.38
MEA vs. REF%		−59.44	−39.47	−30.58	−30.82	+57.04	+14.53	+23.16

Table 8.3 HSDPA Throughput Statistics

<i>Configuration</i>	$\tilde{\phi}(k^*), (kbps)$			$RR \Phi_i(k^*), (kbps)$			$PF \Phi_i(k^*), (kbps)$		
	5%	95%	Mean	5%	95%	Mean	5%	95%	Mean
REF	458.38	1548.68	959.45	601.92	1320.69	932.94	646.69	1364.58	987.58
MT	676.92	1914.45	1175.51	866.87	1419.88	1146.25	903.63	1453.06	1193.56
ET	738.65	2033.55	1248.46	935.98	1448.16	1204.04	973.64	1496.81	1249.10
AZ	506.88	1616.08	1011.71	651.91	1366.55	984.71	687.55	1402.18	1038.77
MEA	750.59	2010.63	1248.85	965.55	1495.23	1215.33	982.28	1519.09	1261.18
MEA vs. REF%	+63.75	+29.83	+30.16	+60.41	+13.22	+30.27	+51.89	+11.32	+27.70

The optimized configurations have also been compared to that obtained by minimizing uniform CPICH power in [19]. Interestingly, the approaches demonstrate very similar single-user HSDPA performance, that is, optimizing antenna configuration using CPICH as the objective and defining bottleneck pixel as the one requiring the highest CPICH power [19] give a good solution for HSDPA throughput. CPICH minimization, however, results in a larger variation in cell sizes due to not taking into account the traffic amount in cells. Large cells have a negative impact when the cell HSDPA performance or user performance at a higher layer is evaluated, as these cells diminish the gain obtained from more HSDPA power available in cells. The solution obtained from HSDPA throughput optimization with the UL coverage constraint, on the other hand, has a higher CPICH power, but more balanced cell sizes.

Finally, we investigate a trade-off between the gain from configuration optimization and the amount of efforts needed to configure the network in terms of the number of cells that require reconfiguration. For each optimized configuration, we collect the information during the optimization search in which uniform HSDPA service demand is assumed. The results are shown in Figure 8.8. Statistics for improving moves only have been

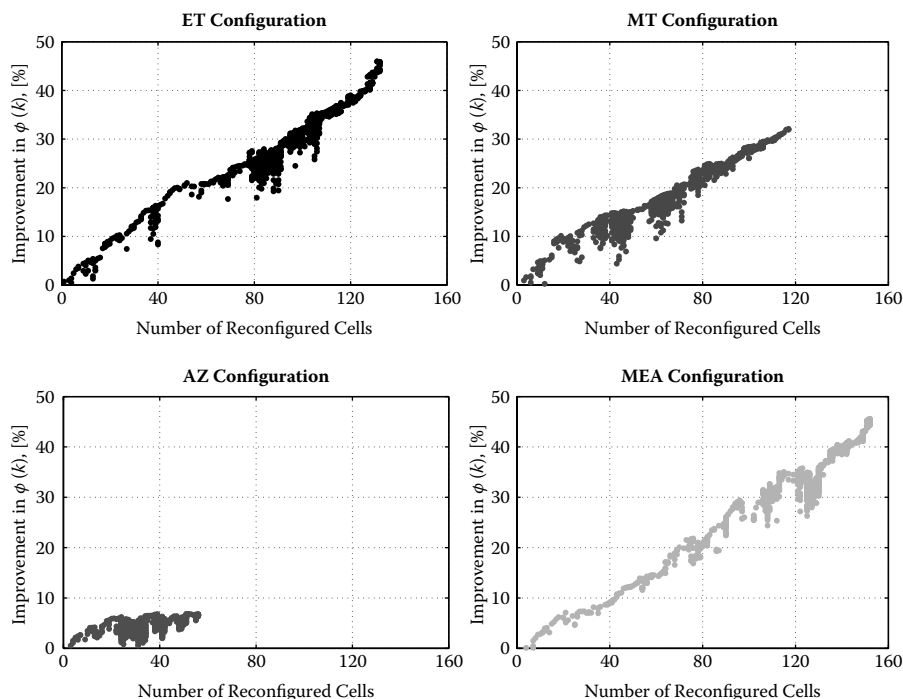


Figure 8.8 Single-user HSDPA throughput improvement versus the number of reconfigured cells.

saved. Recall, however, that accepting worse solutions and moving from those is allowed with simulated annealing. Note also that the number of reconfigured cells does not necessarily increase with the number of search iterations, and points with the same number of reconfigured cells may or may not correspond to the same set of cells. In addition to earlier noted higher gain with electrical tilting, we make the following observations. The Pareto 20/80 rule, by which 20% of efforts gives 80% of the result, seems to not apply to network reconfiguration in our case study where the gain increases almost linearly with the number of cells involved, although a concave shape in the left part of the curves can still be observed. It becomes evident that network optimization is a complex task and simple cell-by-cell tuning is not likely to lead to the desired result. Also, once configured, re-planning a network can be a very costly procedure for an operator, which motivates for using advanced radio network planning tools with large-scale automated optimization capabilities already in earlier network planning stages.

8.6 Conclusions

An optimization framework for automated HSPA cell planning was presented in this chapter, including a detailed system model and an optimization algorithm that is particularly efficient for large network optimization. Moreover, the modeling approach is well-suited for planning networks in heterogeneous environments because the optimization framework does not make any restriction on cell structure or radio propagation characteristics. Our numerical experiments for a realistic case study demonstrate that the presented optimization approach can provide a significant gain in HSPA performance, especially at the cell edge. More efficient radio resource utilization, network performance gain, higher service quality, and improved user satisfaction are the other benefits of a well-planned radio network. These, combined with the complexity consideration of the planning task, the amount of work and reconfiguration cost for improving a poorly planned network, highly motivate for using automated radio network optimization.

References

- [1] 3GPP, Requirements for Support of Radio Resource Management (FDD), 3GPP TS 25.133 V8.5.0, 2008.
- [2] 3GPP, Physical Channels and Mapping of Transport Channels onto Physical Channels (FDD), 3GPP TS 25.211 V8.3.0, 2008.

- [3] IST-2000-28088 MOMENTUM Project, <http://momentum.zib.de>, 2005.
- [4] E. Aarts and J. K. Lenstra (Eds.), *Local Search in Combinatorial Optimization*, Princeton University Press, 2003.
- [5] A. Eisenblätter and H.-F. Geerdes, Wireless network design: Solution oriented modeling and mathematical optimization, *IEEE Wireless Commun. Mag.*, 13(6): 8–14, 2006.
- [6] A. Eisenblätter, A. Fügenschuh, E.R. Fledderus, H.-F. Geerdes, B. Heideck, D. Junglas, T. Koch, T. Kürner, and A. Martin, Mathematical methods for automatic optimization of UMTS radio networks, Project Report D4.3, IST-2000-28088, MOMENTUM, 2003.
- [7] F. Frederiksen, H. Holma, T. Kolding, and K. Pedersen, HSDPA bit rates, capacity, and coverage, in H. Holma and T. Toskala (eds.), *HSDPA/HSUPA for UMTS: High Speed Access for Mobile Communication*, John Wiley & Sons, 2006.
- [8] M.R. Garey and D.S. Johnson, *Computers and Intractability: A Guide to the Theory of NP-Completeness*, W.H. Freeman, 1979.
- [9] F. Glover and M. Laguna, *Tabu Search*, Kluwer Academic Publishers, 1997.
- [10] D.E. Goldberg, *Genetic Algorithms in Search, Optimization and Machine Learning*, Kluwer Academic Publishers, 1989.
- [11] H. Holma, T. Kolding, K. Pedersen, and J. Wigard, Radio resource management, in H. Holma and T. Toskala (Eds.), *HSDPA/HSUPA for UMTS: High Speed Access for Mobile Communication*, John Wiley & Sons, 2006.
- [12] H. Holma, K. Pedersen, and J. Reunanen, Radio resource management, in H. Holma and T. Toskala (Eds.), *WCDMA for UMTS: HSPA Evolution and LTE*, John Wiley & Sons, 2007.
- [13] S. Kirkpatrick, C.D. Gelatt, and M.P. Vecchi, Optimization by simulated annealing, *Science*, 220(4598): 671–680, 1983.
- [14] J. Laiho, A. Wacker, and T. Novasad (Eds.), *Radio Network Planning and Optimisation for UMTS*, John Wiley & Sons, 2002.
- [15] Z. Michalewicz and D.B. Fogel, *How to Solve It: Modern Heuristics*, Springer-Verlag, 2004.
- [16] M. Nawrocki, H. Aghvami, and M. Dohler (Eds.), *Understanding UMTS Radio Network Modelling, Planning and Automated Optimisation: Theory and Practice*, John Wiley & Sons, 2006.
- [17] M.G.C. Resende and C.C. Ribeiro, Greedy randomized adaptive search procedures, in F. Glover and G. Kochenberger (Eds.), *Handbook of Metaheuristics*, pp. 219–249, Kluwer Academic Publishers, 2003.
- [18] I. Siomina, Radio Network Planning and Resource Optimization: Mathematical Models and Algorithms for UMTS, WLANs, and ad hoc Networks, Ph.D. dissertation, Linköping University, LiU-Tryck, 2007.
- [19] I. Siomina, P. Värbrand, and D. Yuan, Automated optimization of service coverage and base station antenna configuration in UMTS networks, *IEEE Wireless Commun. Mag.*, 13(16): 16–25, 2006.